Thin Solid Films 599 (2016) 78–83

Contents lists available at ScienceDirect

Thin Solid Films

journal homepage: www.elsevier.com/locate/tsf

Optimization of the post-deposition annealing process of high-mobility In_2O_3:H for photovoltaic applications

H. Scherg-Kurmes [a,*], S. Seeger [d], S. Körner [a], B. Rech [c], R. Schlatmann [b], B. Szyszka [a]

[a] Technische Universität Berlin, Einsteinufer 25, 10587 Berlin, Germany
[b] Helmholtz-Zentrum Berlin für Materialien und Energie GmbH, PVcomB, Schwarzschildstraße 3, 12489 Berlin, Germany
[c] Helmholtz-Zentrum Berlin für Materialien und Energie GmbH, Institute Silicon Photovoltaics, Kekuléstr. 5, 12489 Berlin, Germany
[d] Optotransmitter-Umweltschutz-Technologie e.V., Köpenicker Straße 325, 12555 Berlin, Germany

ARTICLE INFO

Article history:
Received 1 September 2015
Received in revised form 16 December 2015
Accepted 22 December 2015
Available online 24 December 2015

Keywords:
In_2O_3:H
TCO
High mobility
Flash lamp annealing
Crystallization

ABSTRACT

High-mobility hydrogen-doped indium oxide In_2O_3:H (IOH) were deposited by magnetron sputtering (radio frequency 13.56 MHz) from an In_2O_3 target in $Ar/O_2/H_2O$ gas mixtures onto unheated substrates. The as-deposited films were amorphous as shown by X-ray measurements and were crystallized in a post-annealing step in vacuum and air at 180 °C for 15 min. The optical, electrical, and morphological properties as well as the crystallization behavior of these transparent conductive oxides films were investigated in detail. A dependence of the annealing behavior in air on the total pressure during deposition could be shown. High carrier mobilities >100 cm^2/Vs allow for very low optical absorption and a low resistivity around 350 μΩcm. Amorphous IOH films were crystallized by short-term flash lamp annealing (FLA) in argon atmosphere for around 2.7 ms. Spatial temperature distributions in a typical layer stack (crystalline silicon, amorphous silicon, silicon oxide, and IOH film) were calculated within milliseconds after the FLA-treatment. Electron backscattering diffraction measurements of IOH films crystallized by FLA reveal a polycrystalline microstructure with an average lateral crystallite size of 333 nm. The crystallization process of these IOH films was studied by XRD and Hall measurements.

1. Introduction

Transparent conductive oxides (TCOs) are employed as contact layers thin film solar cells. They transmit incoming light to the absorber and conduct the generated charge carriers laterally to the metal contacts. Thus, the TCO should have a high optical transparency as well as a high electrical conductivity to ensure good solar cell performance. The free charge carriers, which are necessary for the electrical conductivity, also cause free carrier absorption in the near infrared (NIR) spectrum. In order to fulfill the two conflicting requirements mentioned above, it is necessary to reduce the free carrier density and increase the carrier mobility in the TCO at the same time. By accomplishing this, high optical transparency can be achieved while still maintaining a good electrical conductivity.

Increasing the transparency of the TCO increases the short-circuit current density (J_{sc}) in solar cells. Hydrogen-doped indium oxide In_2O_3:H (IOH) has been widely discussed as a suitable TCO for this purpose, because of its mobility higher than 100 cm^2/Vs [1–4]. Very low optical absorption can be achieved with this material at resistivities around 350 μΩcm. By introducing a small amount of water vapor into the sputtering chamber during the deposition, IOH films can be deposited in X-ray-amorphous state and crystallized in a post-deposition annealing step lasting usually 15–30 min at approx. 180 °C in vacuum, as has been shown in our previous work [5].

The development of amorphous In_2O_3:Sn (ITO) by adding water vapor or H_2 to the sputtering gas has been shown in literature [6,7]. The crystallization behavior of hydrogenated ITO is similar to IOH. Ando *et al.* show that the growth of crystallites in the ITO film is suppressed by the addition of water vapor during the sputtering process at room temperature [6]. After a post-deposition annealing step, the films crystallized to polycrystalline structures. Betz *et al.* also achieved suppression of crystal growth during ITO deposition at room temperature by adding H_2 to the sputtering gas [7]. They showed that the amorphous ITO film reaches almost the same resistivity after a post-deposition annealing step as an ITO film which is deposited in polycrystalline phase at 200 °C substrate temperature. In our previous publication, we demonstrated that IOH has a lower absorption in the NIR spectrum than ITO due to its lower free carrier concentration and higher mobility [5], and thus has the possibility to reach a higher J_{SC} in solar cells than ITO.

We synthesized IOH films using rf magnetron sputtering from a ceramic In_2O_3 target in $Ar/O_2/H_2O$ gas mixtures. The crystallization of amorphous IOH films was analyzed using various annealing treatments in vacuum, air, and argon gas atmosphere.

* Corresponding author.
E-mail address: h.scherg-kurmes@tu-berlin.de (H. Scherg-Kurmes).

http://dx.doi.org/10.1016/j.tsf.2015.12.054
0040-6090/

In our previous work, we have shown that oven annealing in vacuum at 180 °C for periods longer than 10 min decreases the open-circuit voltage (V_{OC}) of a-Si:H/c-Si heterojunction cells, because of a degradation of the passivating a-Si:H layer [5]. Improved V_{OC} values can be achieved by annealing heterojunction cells in air at 200 °C for ≤10 min [5,8]. Therefore, we investigated the effect of annealing in air on IOH films deposited at different process pressures.

Also for CIGS cells, a degradation of the solar cell parameters has been shown due to an annealing process for 2 h at 180 °C in vacuum [9]. In this paper, we performed very short-term flash lamp annealing (FLA) to crystallize amorphous IOH films within 2.7 ms in argon gas atmosphere at 5×10^4 Pa. The extremely short duration of FLA reduces thermal stress on heat-sensitive substrates like CIGS cells and may provide an approach to benefit from the high transitivity of an IOH-front-contact without degrading the cells during the annealing process. Finally, both annealing in air and FLA have the potential to reduce processing costs compared to the conventional vacuum annealing step.

2. Experimental details

The IOH films were deposited by rf (13.56 MHz) magnetron sputtering from a ceramic In_2O_3 target onto unheated substrates. Hydrogen doping was realized by connecting a reservoir filled with deionized water via manual needle- and blocking-valves to the sputtering chamber (Roth&Rau). Prior to the deposition process, the H_2O partial pressure was set by adjusting the needle valve manually. Approximately 15 min were required to stabilize the H_2O partial pressure. The sputtering system contains three 2-inch targets and is capable of sputtering IOH, ITO, and AZO which were protected by a shutter. The substrates were placed on a rotatable silicon carrier and oscillate under the target.

The base pressure of the sputtering system is approx. 3.7×10^{-5} Pa. We used an oxygen partial pressure of 0.32% (2.6 sccm of 2.5% Ar/O_2 gas mixture and 18 sccm of Ar). The water partial pressure p_{H2O} was varied between 1.6×10^{-4} Pa and 10^{-2} Pa. RF power was set to 70 W, and the total pressure was varied between 0.15 and 0.6 Pa. After deposition, the samples were annealed under varying conditions. Vacuum annealing was performed in the sputtering chamber under vacuum at $T_a = 180$ °C for 2 h. Annealing in air was performed on a titanium hot plate set to 200 °C in room atmosphere. Flash lamp annealing was performed using a commercially available xenon flash lamp annealing system (DTF FLA 100) in a vacuum chamber in argon atmosphere at about 5×10^4 Pa.

All samples we used for the FLA experiments had the following layer stack (top to bottom): 155 nm IOH / 200 nm SiO_x / 20 nm a.Si:H / 280 µm c-Si. To perform the Hall measurements, we electrically separated the IOH films from the Si substrate by depositing a 200 nm SiOx interlayer. This was necessary to eliminate Si influence on the Hall measurements of the IOH films. For the annealing experiments in vacuum and air, we used IOH films on glass with a film thickness of 70 nm in order to reduce the processing time of the deposition process. For the FLA experiments, we increased the IOH film thickness to 155 nm in order to achieve a better signal-to-noise ratio for the X-ray diffraction (XRD) measurements.

XRD scans were performed with a PANalytical–XPert MRD and a Bruker D2-Phaser system in Bragg–Brentano geometry. The optical measurements were collected using a Perkin Elmer Lambda 1050 dual-beam spectrophotometer with an integrating sphere. The film thickness was determined by spectroscopic ellipsometry measurements using a Sentech 850 ellipsometer, and fitting optical Leng-Drude oscillator models to the measured data. The measurement error for the film thickness measurements was approx. ±2.5%. Hall measurements were performed using an Ecopia HMS-3000 system in van der Pauw geometry with a measurement error of approx. ±2.5%. The carrier density and resistivity of the films displayed in Fig. 1 and Fig. 2 are calculated using both the hall- and film-thickness measurements, and therefore have a measurement error of ±5%. The mobility is calculated directly from the hall measurements with a measurement error of ±2.5%.

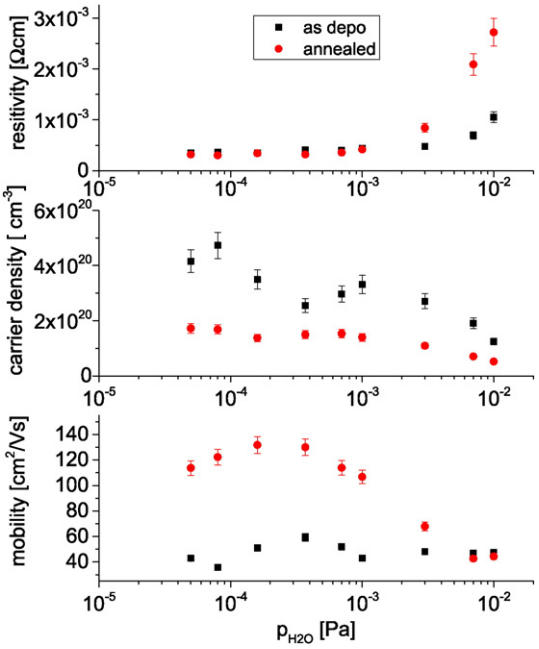

Fig. 1. Resistivity, carrier density, and carrier mobility as a function of water partial pressure for as-deposited and annealed 70 nm IOH films on glass determined by Hall measurements in van der Pauw geometry.

J–V measurements were carried out using a Wacom-155S-L2 solar simulator. Scanning electron microscopy (SEM) and electron backscatter diffraction (EBSD) measurements were performed with a Hitachi S4100 SEM.

Short-term annealing of the IOH films was performed using four xenon flash lamps (160 mm length), which provide single pulses of high-energetic light in the spectral range from 200 to 1000 nm with a broad maximum around 450 nm. Energy density and pulse length of the flash light were adjusted by the capacitance and the inductance of an LC circuit. The pulse length was set to about 2.7 ms. The energy density was defined via the charging voltages of the capacitor.

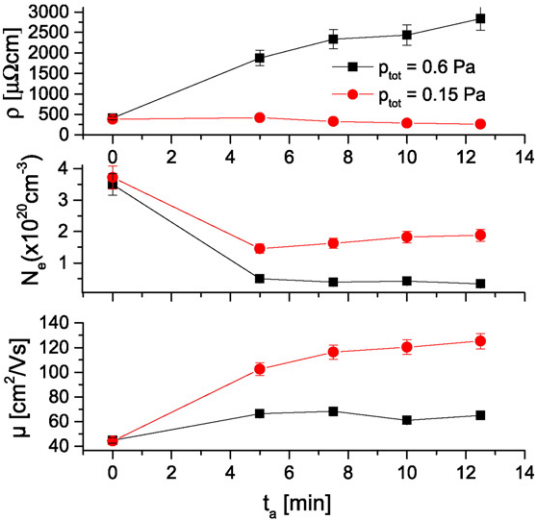

Fig. 2. Results of Hall measurements performed in van der Pauw geometry on 70 nm thick IOH films on glass. The total pressure during deposition was varied (squares: $p_{tot} = 0.6$ Pa, circles $p_{tot} = 0.15$ Pa). After deposition, the films were annealed in air for varying times.

3. Results and discussion

In order to evaluate the influence of hydrogen doping on the ratio of the crystalline phase in the IOH films, XRD scans of undoped and hydrogen-doped In_2O_3 films were compared in our previous work [9]. Undoped In_2O_3 films grow polycrystalline when they were deposited by rf magnetron sputtering at room temperature. By introducing water vapor into the sputtering chamber during the deposition, —OH molecules were incorporated, and the film grew amorphously. In a post-deposition annealing step, the films were crystallized.

It has been shown that the crystallites of the post-annealed film are larger than those of the undoped In_2O_3, thus enabling the higher carrier mobility [1]. The hydrogen content in the doped IOH films has been measured by Koida *et al.* by thermal desorption spectroscopy to be approx. 3 at.% at $p_{H2O} = 10^{-4}$ Pa before and after annealing [1].

In the literature, the mechanics of amorphous In_2O_3:H growth due to water vapor in the sputtering chamber have been explained [6,10]: water vapor is split into H and —OH with a dangling bond by the plasma. —OH prevents the formation of In—O bonds in the growing film, forming In—OH instead and inhibiting the crystallization of the film. Another effect of —OH in the film is the termination of oxygen vacancies, thus decreasing the free carrier density in the film. At annealing temperatures >150 °C, the In—OH bonds are broken and the formation of In—O bonds leads to the growth of large crystallites. H^+ remains in the In—O matrix as a donor, as has been shown by Limpijumnong *et al.* [11].

Hall measurements were performed on IOH films in as-deposited and annealed (2 h at 180 °C in vacuum) state, which were prepared at water vapor partial pressures from 8×10^{-5} to 10^{-2} Pa (see Fig. 1). During annealing, the carrier density (N_e) decreases from approx. 3×10^{20} cm^{-3} to approx. 1×10^{20} cm^{-3}, probably due to the healing of oxygen vacancies in the In_2O_3 lattice. At $p_{H2O} = 9 \times 10^{-5}$ Pa… 3×10^{-4} Pa, the mobility (μ_H) increases during annealing from 40 to up to 130 cm^2/Vs due to the crystallization of the films and because of decreased impurity scattering [1]. In this p_{H2O} range, films with resistivities lower than 300 μΩcm were implemented. These values agree well with the results shown in literature [1,10,12].

If p_{H2O} was raised above 10^{-3} Pa, the carrier densities for the annealed films decrease to very low values <10^{19} cm^{-3}, while the mobilities also decrease below 60 cm^2/Vs. This leads to IOH films with resistivities higher than 2500 μΩcm. We assume that due to the high p_{H2O}, larger amounts of —OH and H_2O are incorporated into the indium oxide lattice. During the annealing process of the IOH films, these molecules hinder the crystallization and increase impurity scattering, and therefore reduce the mobility. Additionally to the decrease in carrier density due to the healing of oxygen vacancies during annealing, a certain amount of —OH probably remains in the IOH film at high p_{H2O}, thus further decreasing N_e to values <10^{19} cm^{-3} by terminating even more oxygen vacancies. This explains the high resistivities observed for annealed IOH films deposited at high p_{H2O}. We can conclude that a beneficial effect of doping In_2O_3 with water vapor can only be observed up to $p_{H2O} = 10^{-3}$ Pa. Above this partial pressure, impurity scattering and the termination of oxygen vacancies probably caused by excess —OH in the films lead to increased resistivities.

In our previous work [5], we showed that the post-deposition annealing step at 180 °C in vacuum, which is usually used to crystallize the IOH films on a-Si:H/c-Si heterojunction cells, reduced the open-circuit voltage V_{OC} due to the degradation of the a-Si:H passivation layer. An annealing step for 5 min at 200 °C in air increases V_{OC} by 10–20 mV. Fig. 2 depicts the results of Hall measurements on 70 nm thick IOH films on glass. The total pressure during deposition was varied (squares: $p_{tot} = 0.6$ Pa, circles $p_{tot} = 0.15$ Pa). In the as-deposited state, both films exhibit similar electrical properties, shown in the diagram at the annealing time $t_a = 0$. After the deposition, the films were annealed in air for varying times. If IOH films were deposited at the higher total pressure ($p_{tot} = 0.6$ Pa), a decrease of the carrier density (N_e) to the 10^{19} range can be observed after $t_a = 5$ min. The longer the annealing time, the more decreases N_e, which causes a high resistivity up to 3000 μΩcm. We attribute the high resistivity to oxygen migration into the film during annealing. The mobilities (μ_H) of the films deposited at high p_{tot} remain below 70 cm^2/Vs. High mobilities and low resistivities for IOH films grown at high p_{tot} can only be achieved by annealing in oxygen-free atmosphere or vacuum [5]. By lowering the deposition pressure to 0.15 Pa, N_e remains over 1.5×10^{20} cm^{-3}, and μ_H increases up to 120 cm^2/Vs, delivering resistivities around 300 μΩcm. According to Thornton's structure zone model, the density of the film increases with lower process pressure [13]. It can be assumed that the higher film density prevents oxygen migration, hence the resistivities decrease during the annealing process. In literature, μ > 120 cm^2/Vs has been reached for IOH films on glass deposited at $p_{tot} = 0.66$ Pa, which have been annealed in air for 15 min despite the high total pressure [3]. The discrepancy to the results measured in this work can probably be explained by a difference in the sputtering system setups and the sputtering power density.

By using IOH films deposited at a low p_{tot} as front TCO for a-Si:H/c-Si heterojunction cells, the technologically complicated annealing step in vacuum could be circumvented. By annealing the cells in air, we were also able to increase the V_{OC} of the cells up to 720 mV (compared to 700 mV reached by vacuum annealing, as shown in our previous work [5]).

Annealing steps in the photovoltaic industry require fast processing time, low energy consumption, and low-cost non-vacuum processing. Therefore, we investigated the crystallization of the amorphous IOH films by using a short-term flash lamp annealing (FLA) in argon atmosphere. Since the FLA occurs within several milliseconds, it is a promising technology for thermal annealing of temperature-sensitive substrates, interlayers, or devices, e.g., the a-Si:H layer in H-J solar cells.

The absorbing materials of the layer stack, a-Si:H(i) and c-Si(p), were heated due to the light pulse, since the IOH top layer and SiO_2 layer are almost transparent. The IOH films were heated up mainly due to thermal conductivity within the layer stack. The pulse length and energy density, preheating temperature and heat transfer, as well as the physical properties of the materials, e.g. thermal conductivity, specific heat and density, determine the maximum temperature in the IOH films. Additionally, the flat sample surface reflects the light pulse. Therefore, the spectral reflectance was taken into account when calculating the temperature distribution. The spatial and time-dependent temperature distributions in a typical layer stack were calculated by using finite element simulation software (Comsol 4.2a). Fig. 3 shows

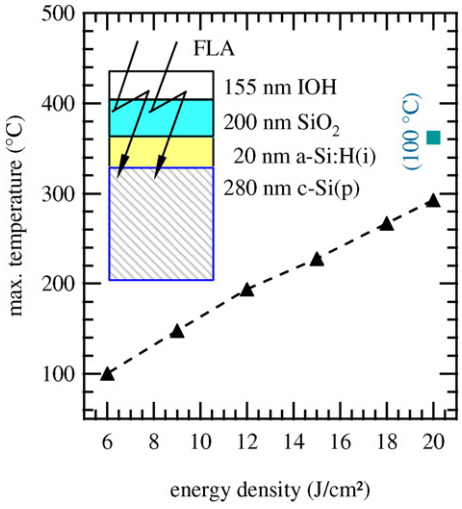

Fig. 3. Calculated temperatures of the IOH layer in dependence on the energy density of the xenon flash light without and with preheating. The inset depicts the layer stack schematically, i.e., 155 nm IOH / 200 nm SiOx / 20 nm a.Si:H / c-Si.

the computed temperature of the IOH layer in dependence on the energy density of the xenon flash light. The inset in Fig. 3 depicts the layer stack schematically, i.e., 155 nm IOH / 200 nm SiO_x / 20 nm a.Si:H / c-Si. For the highest energy density (20 J/cm²) the calculation gives 290 °C (unheated substrate) and the temperature increases over 360 °C, if the silicon wafer was supplementally heated during the flash annealing.

Fig. 4 shows three annealing experiments (15 J/cm², 20 J/cm², and 20 J/cm² at 100 °C). The computed temperature distribution at the surface of the IOH layer (solid lines) and the backside of the c-Si(p) wafer (dotted lines) and the intensity of the flash light pulse are plotted versus time (see the grey-filled shape). The temperature of the IOH layer increases within 3 ms in the whole layer stack. After the light pulse, the layer stack cools rapidly down due to the surface-to-ambient radiation. The cooling curve of the samples was measured with a thermocouple (see Fig. 4). The temperature of the sample drops below 200 °C after a time of about 11 s even if the sample was preheated up to 100 °C.

In our previous work, we have shown that IOH films crystallize rapidly once the annealing temperature exceeds 150 °C [5]. In Fig. 5, XRD measurements of the test samples are shown. Already in as-deposited state, two peaks originating from the SiO_2 layer in the substrate are visible at 33° and 62°. These peaks are of no consequence to the crystallinity of IOH and can be ignored in the following explanations. The Hall mobility of each film was measured after annealing and is shown above each curve. Up to a flash lamp energy of 12 J/cm², no In_2O_3 XRD peaks can be seen, and the Hall mobility does not increase compared to the as-deposited film. This indicates that the flash energy was not sufficient to crystallize the film, so that the film is still in amorphous phase. At 15 J/cm², a very small In_2O_3 <222> peak is visible, and the Hall mobility increases to 55 cm²/Vs, indicating a partially crystallized IOH film. At 18 and 20 J/cm², which was the maximum flash energy of the FLA system, the <222> peak intensity increases, although the Hall mobility was 54 cm²/Vs and the film was not fully crystallized. By preheating the sample by infrared radiation heaters to 100 °C and then flashing with 20 J/cm², we were able to fully crystallize the IOH film and reach a mobility of 112 cm²/Vs. Infrared-preheating to 100 °C without FLA did not crystallize the IOH films, because 100 °C is still below the crystallization temperature of 150 °C.

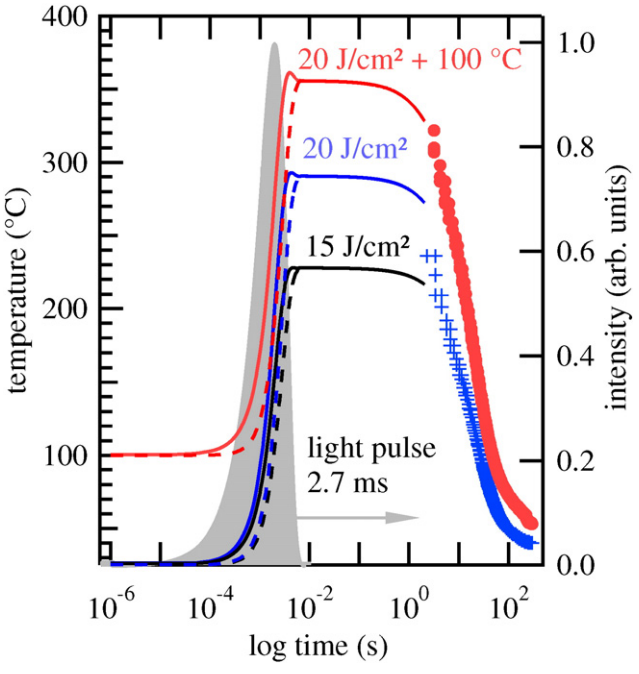

Fig. 4. The time-dependent temperature distribution at the surface of the IOH layer (solid lines) and the backside of the c-Si(p) wafer (dotted lines) are plotted for three annealing experiments (15 J/cm², 20 J/cm², and 20 J/cm² at 100 °C). The time-dependent intensity of the flash light pulse is depicted as the grey-filled shape (see right axis). The blue and red markers represent the measured temperatures during the cooling of the samples.

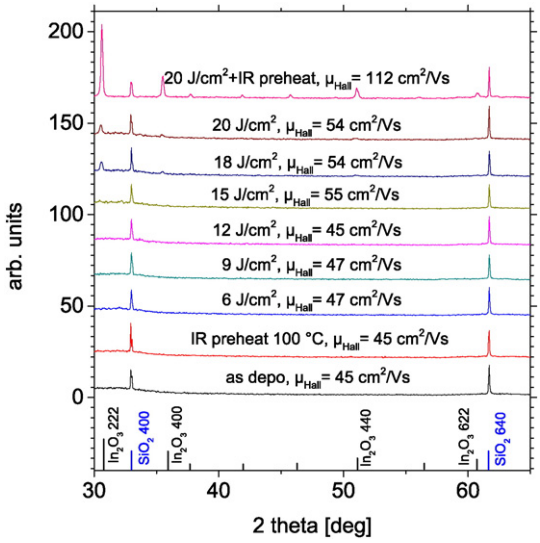

Fig. 5. XRD measurements of 155 nm IOH films on SiO_x / a-Si:H / c-Si substrates flash-annealed at different flash energies. The hall mobility of the annealed films is shown at each curve. At the bottom of the diagram, the powder spectrums of In_2O_3 and SiO_2 are displayed.

Fig. 6a shows the EBSD map giving the orientation distributions of a partially crystallized IOH film (t = 155 nm) on a SiO_x/a-Si:H/c-Si substrate. This sample was annealed by 18 J/cm² FLA in Ar. The black areas represent the amorphous phase of IOH. Surrounded by the amorphous phase, small, scattered crystallites are visible. The energy of the flash was insufficient to fully crystallize this IOH film, also in accordance

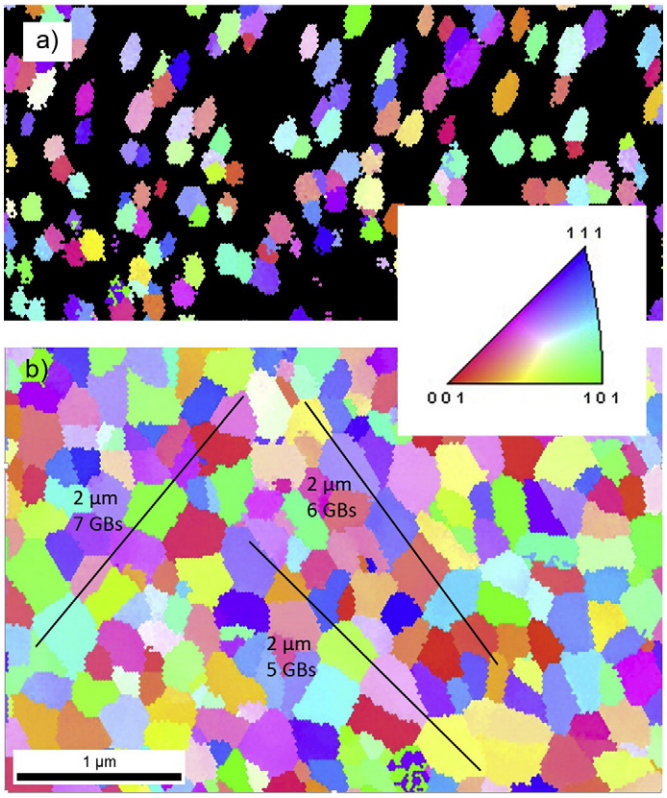

Fig. 6. EBSD map of a) IOH on SiOx/a-Si:H/c-Si after 18 J/cm² FLA. b) IOH on SiOx/a-Si:H/c-Si after 100 °C IR preheat + 20 J/cm² FLA. The average lateral crystallite size is 333 nm and was calculated along the 3 black lines shown in the figure.

with the XRD measurements (see Fig. 5). Fig. 6b shows the EBSD mapping of a fully crystallized IOH film (t = 155 nm) on a SiO_x/a-Si:H/c-Si substrate, preheated up to 100 °C by the IR heater and annealed with a energy density of 20 J/cm^2. Fig. 6b shows only randomly oriented compact crystal structure without amorphous phases. The average lateral crystallite size L was calculated along the three black lines shown in Fig. 6b. The total line length (3 × 2 μm) was divided by the number of grain boundaries crossed by the lines (7 + 5 + 6 = 18), which yields L = 6 μm/18 = 333 nm.

The spectral reflectivity of three samples is shown in Fig. 7. The reflectivity of as-deposited IOH is compared to IOH films annealed by 100 °C IR preheating + 20 J/cm^2 FLA and IOH films conventionally annealed for 30 min at 180 °C in vacuum.

The oscillations which can be observed in the spectra are mainly due to interfering reflections from IOH and the SiO_x, a-Si:H an c-Si layers beneath it. It has been shown that the plasma edge of IOH films in as-deposited state with $N_e \approx 3.5 \times 10^{20}$ cm^{-3}, at which the reflectivity begins to rise continually, is located approx. at 1600 nm [1]. In Fig. 7, this rise of the reflectivity caused by the plasma edge is superimposed over the interferences caused by the stack of films beneath the IOH. Therefore, we can assume that for the as-deposited sample, the rise in reflectivity beginning at 1600 nm is caused by the plasma edge of the IOH film. It has been shown that for IOH films annealed for 2 h in vacuum with $N_e \approx 1.5 \times 10^{20}$ cm^{-3}, the plasma edge is shifted close to 2500 nm [10]. After annealing the IOH samples in vacuum as well as by FLA, the carrier density decreases (see Table 1). Consequently, the change in the spectra of the annealed IOH films compared to the as-deposited film can be explained by the shift of the plasma edge to longer wavelengths. The reflection spectra of the IOH films annealed in vacuum and by FLA are reasonably close to one another. This shows that no degradation of the optical properties in the visible and NIR spectrum of the films is caused by FLA annealing compared to vacuum annealing.

Table 1 compares the carrier densities N_e, the mobilities and the resistivities of the as-deposited IOH film with that of two annealed IOH films, conventionally annealed in vacuum (30 min at 180 °C) and short-term annealed in argon (FLA 20 J/cm² and 100 °C).

The carrier density of the film annealed by FLA is a little higher than for film annealed for 30 min in vacuum. Except for this difference, the optical and electrical properties of the films annealed by conventional annealing (30 min at 180 °C in vacuum) and FLA are quite similar. This confirms that the conventional IOH annealing step for approx. 30 min in vacuum can be replaced by a FLA step lasting only 2.7 ms without losses in the annealed IOH film properties.

The samples we used for the FLA experiments were deposited on flat c-Si wafers and had a relatively high reflectivity. In order to adapt the FLA process for IOH films on optimized solar cell stacks with lower reflectivity because of light trapping, the higher percentage of absorbed radiation has to be taken into account. As less radiation is reflected by the solar cell stack, the flash energy can be reduced, and the IR preheating step is no longer necessary to reach temperatures above the crystallization temperature of 150 °C in the IOH film.

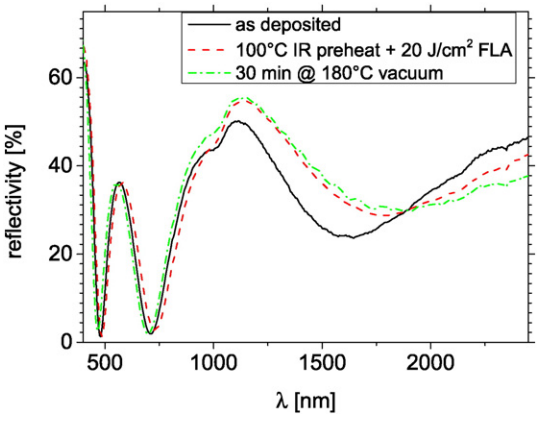

Fig. 7. Reflectivity of c-Si/a-Si/SiOx/IOH test structures. Data for as-deposited, standard-annealed, and flash-annealed samples are shown.

Table 1
Hall measurements of IOH films in as-deposited state compared to IOH films annealed by IR preheating + FLA at 20 J/cm^2 and conventional annealing for 30 min at 180 °C in vacuum.

	Ne [cm^{-3}]	μ [cm²/Vs]	ρ [μOhm*cm]	t [nm]
IOH (as deposited at 25 °C)	3.45E+20	48	380	155
IOH (IR preheat + FLA 20 J/cm^2)	2.11E+20	112	263	155
IOH (annealed 30 min at 180 °C in vacuum)	1.68E+20	117	319	155

4. Conclusion

In conclusion, we systematically investigated the effect of the water vapor partial pressures p_{H2O} on the electrical properties of IOH films prepared by magnetron sputtering from an In_2O_3 target in argon/oxygen atmosphere, subsequently annealed in vacuum and air at 180 °C. The highest mobilities of 130 Vs/cm^2 were achieved between p_{H2O} = 0.1 and 0.3 mPa. These polycrystalline films exhibit large grains (>500 nm) confirmed by EBSD. The crystallization behavior in air atmosphere for IOH films deposited at different total pressures has been investigated. Films deposited at p_{tot} = 0.1 Pa achieve high mobilities after annealing in vacuum as well as in air atmosphere. However, films deposited at a higher total pressure p_{tot} = 0.6 Pa degrade after annealing in air, probably because of their higher porosity, i.e., lower film density.

Flash lamp annealing has been performed on IOH films on SiO_x/a-Si/c-Si test structures. We found that by preheating the sample to 100 °C by IR heater and flashing with 20 J/cm^2 for 2.7 ms, the IOH films fully crystallize and show comparable electrical and optical properties as achieved by conventional oven annealing, i.e. annealing in air for 15 min at 180 °C.

Acknowledgments

The authors would like to thank Carola Klimm for performing the EBSD measurements.

References

[1] T. Koida, H. Fujiwara, M. Kondo, Hydrogen-doped In2O3 as high-mobility transparent conductive oxide, Jpn. J. Appl. Phys. 46 (2007) L685–L687.
[2] T. Koida, H. Fujiwara, M. Kondo, High-mobility hydrogen-doped transparent conductive oxide for a-Si:H/c-Si heterojunction solar cells, Sol. Energy Mater. Sol. Cells 93 (2009) 851–854.
[3] L. Barraud, Z.C. Holman, N. Badel, P. Reiss, A. Descoeudres, C. Battaglia, S.D. Wolf, C. Ballif, Hydrogen-doped indium oxide/indium tin oxide bilayers for high-efficiency silicon heterojunction solar cells, Sol. Energy Mater. Sol. Cells 115 (2013) 151–156.
[4] H. Sai, T. Koida, T. Matsui, I. Yoshida, K. Saito, M. Kondo, Microcrystalline silicon solar cells with 10.5% efficiency realized by improved photon absorption via periodic textures and highly transparent conductive oxide, Appl. Phys. Express 6 (2013) 104101.
[5] H. Scherg-Kurmes, S. Körner, S. Ring, M. Klaus, L. Korte, F. Ruske, R. Schlatmann, B. Rech, B. Szyszka, High mobility In2O3:H as contact layer for a-Si:H/c-Si heterojunction and μc-Si:H thin film solar cells, Thin Solid Films 594 (2015) 316–322.
[6] M. Ando, E. Nishimura, K. Onisawa, H. Minemura, Effect of microstructures on nanocrystallite nucleation and growth in hydrogenated amorphous indium-tin-oxide films, J. Appl. Phys. 93 (2) (2003) 1032–1038.
[7] U. Betz, M. Kharrazi Olsson, J. Marthy, M.F. Escolá, F. Atamny, Thin films engineering of indium tin oxide: large area flat panel displays application, Surf. Coat. Technol. 200 (2006) 5751–5759.
[8] D. Zhang, A. Tavakoliyaraki, Y. Wu, R.A.C.M.M. van Swaaij, M. Zeman, Influence of ITO deposition and post annealing on HIT solar cell structures, Energy Procedia 8 (2011) 207–213.

[9] H. Scherg-Kurmes, S. Koerner, F. Ruske, C. Wolf, R. Muydinov, R. Schlatmann, B. Szyszka, High mobility InOx:H transparent conductive oxide for thin film solar cells, 10th Int. Conf. Coat. Glass Plast 2014, pp. 381–384.
[10] T. Koida, M. Kondo, K. Tsutsumi, A. Sakaguchi, M. Suzuki, H. Fujiwara, Hydrogen-doped In2O3 transparent conducting oxide films prepared by solid-phase crystallization method, J. Appl. Phys. 107 (2010) 033514.
[11] S. Limpijumnong, P. Reunchan, A. Janotti, C.G. Van de Walle, Hydrogen doping in indium oxide: an *ab initio* study, Phys. Rev. B 80 (2009) 193202.
[12] T. Koida, H. Shibata, M. Kondo, K. Tsutsumi, A. Sakaguchi, M. Suzuki, H. Fujiwara, Correlation between oxygen stoichiometry, structure, and opto-electrical properties in amorphous In2O3:H films, J. Appl. Phys. 111 (2012) 063721.
[13] J.A. Thornton, High rate thick film growth, Annu. Rev. Mater. Sci. 7 (1977) 239–260.